PG 1254+047: AN INTRINSICALLY X-RAY WEAK, HEAVILY ABSORBED BALQSO?

Bassem M. Sabra & Fred Hamann
Department of Astronomy, University of Florida, Gainesville, FL 32611
Accepted for publication in the Astrophysical Journal

ABSTRACT

We present *Chandra* observations of the radio-quiet Broad Absorption Line (BAL) QSO PG 1254+047. We find that it is a weak X-ray source, with a total of 44 ± 7 photons measured in 36 ksec across the observed energy range $0.7 - 6.0$ keV. Its X-ray weakness is consistent with the known correlation between $\alpha_{\rm ox}$ and the strength of the UV absorption lines. The spectral energy distribution suggests that PG 1254+047 is intrinsically X-ray weak, in addition to being heavily X-ray absorbed. The X-ray absorption column density is $N_{\rm H} > 10^{23}$ cm^{-2} for neutral gas, while the intrinsic (unabsorbed) emission spectrum has $\alpha_{ox} > 2$. The data are fit best by including an ionized (rather than neutral) absorber, with column density $N_{\rm H} \gtrsim 2 \times 10^{23}$ cm^{-2}. The degree of ionization is consistent with the UV BALs, as is the total column density if the strongest UV lines are saturated. If the X-ray absorber forms in a wind that is radiatively accelerated to the BAL velocities, then the wind must be launched from a radius of about 10^{16} cm with a mass loss rate of ~ 1 M$_\odot$ yr^{-1}.

Subject headings: galaxies: active—quasars: absorption lines—quasars: individual (PG 1254+047)—X-rays: galaxies

1. INTRODUCTION

Almost all quasi-stellar objects (QSOs) are X-ray sources. The reprocessing of the X-rays by intervening matter along the line-of-sight to the QSO imprints informative features on the resulting spectrum (e.g., Turner 1991). X-ray absorption studies provide an important tool to determine the physical and chemical state of the gas associated with QSOs (e.g., Netzer 1996). A subclass of QSOs that have interesting X-ray properties in terms of continuum strength and absorption are the Broad Absorption Line (BAL) QSOs (Foltz et al. 1990; Weymann et al. 1991). They display broad (FWHM $\approx 10,000$ km s^{-1}) absorption lines in the rest-frame ultraviolet (UV), which originate in an outflow of matter from the central engine of the QSO. The outflow velocity may reach up to 0.2 c (Foltz et al. 1983). Determining the relation between the gases producing the X-ray and UV absorption has profound implications for the wind properties, such as geometry, launch radius, acceleration mechanism and mass loss rate (e.g., Mathur, Elvis, & Singh 1995; Murray, Chiang, & Grossman 1995; Hamann 1998).

BALQSOs are also usually X-ray faint, especially in soft X-rays (Brandt, Laor, & Wills 2000). The similarity of BALQSOs and non-BALQSOs in other parts of the spectrum suggest that X-ray weakness is due to heavy absorption. The high ionization state inferred from the UV absorption lines indicates that the X-ray absorbers are not generally neutral; they could be similar to the "warm" absorbers measured frequently in Seyfert 1 galaxies (George et al. 1998; Reynolds 1997).

One major obstacle to understanding the relationship between BALs and the X-ray absorbers has been that the total column densities derived from the BALs (typically $N_H \lesssim 10^{20}$ cm^{-2}, Hamann, Korista & Morris 1993), are 3 or more orders of magnitude less than those deduced from X-rays (cf. Brandt et al. 2000; Gallagher et al. 1999; Green et al. 2001). However, there is now growing evidence that the BALs are much more optically thick than previously realized (Hamann 1998, Arav et al. 1999, Wang et al. 1999), and therefore the total column densities in *outflowing* BAL gas may be as large as the X-ray absorbers. The correlated appearance of UV and X-ray absorption features (Brandt et al. 2000) shows clearly that the two absorbers are (somehow) physically related. A key question now is whether these features are manifestations of the same gas.

In this paper, we discuss Chandra X-ray observations of PG 1254+047. This object shows BALs ($z_{abs} = 0.870$) that are blueshifted with respect to the systemic velocity of the QSO ($z_{em} = 1.024$). It is also characterized by being an X-ray faint source (Wilkes et al. 1994). Hamann (1998) used the relative strengths of the BALs in this source to show that 1) most of the lines are saturated and, 2) the total column density is *at least* $N_{\rm H} \approx 10^{22}$ cm^{-2}. Those results probably apply generally to BALQSOs, but PG 1254+047 is of particular interest because its BALs are "detached" from the emission lines — appearing at blueshifted velocities from ∼15,000 to ∼27,000 km s^{-1}. If there is a high column density X-ray absorber in this source that can be identified with the BAL gas, then that X-ray absorber must also be outflowing at minimally $15,000$ km s^{-1}. Such a finding would substantially impact the derived mass loss rates and place severe constraints on models of the wind acceleration (Hamann 1998; Hamann & Brandt 2001). Our aim here is to determine the properties of the X-ray spectrum, search for signs of absorption, and define the relationship between the UV and X-ray absorbing gas.

2. OBSERVATIONS AND DATA REDUCTION

PG 1254+047 was observed by *Chandra* using the Advanced Imaging Spectrometer (ACIS) on 29 May 2000. The most recent re-processed (29 February 2001) data released by the Chandra X-ray Center were used. No fil-

tering for high background or bad aspect times was done because the light curves did not show any flare-ups in the count rate and the aspect was a smooth dither pattern with no outlying points. Data extraction and calibration was done using version 1.4 of the Chandra Interactive Analysis of Observations (CIAO). The X-ray analysis package XSPEC (Arnaud 1996) was used for rebinning and spectral analysis. We created the response matrix and ancillary response files by relying on calibration data provided when the chip temperature during observations was -120° C.

We extracted the source counts from a circular region of radius of $5''$ while the background region was an annulus with radii between $10''$ and $20''$, both centered on the position of PG 1254+047. The ACIS image is shown in Figure 1. As determined from the ACIS image, the position of PG 1254+047 is $\sim 1''$— comparable to the spatial resolution of ACIS — from the optical position of the source (α(J2000) = $12^h56^m59.96^s$, δ(J2000) = $04^\circ27'34.2''$, Gould, Bahcall, Maoz 1993). The mere fact of actually detecting PG 1254+047 in X-rays is notable because BALQSOs are expected to be extremely weak in X-rays (Brandt et al. 2000). We obtained a total of 44 ± 7 counts in an effective exposure time of 36 ksec across the observed energy range $\sim 0.7 - 6.0$ keV.

3. ANALYSIS AND RESULTS

We want to understand the reason behind the low count rate: Is it due to intrinsic absorption, intrinsic X-ray weakness, or both? Given the paucity of photons detected, our approach is that of elimination, starting with the simplest model and increasing the level of complexity only after exhausting all means to satisfactorily fit the data with a given model. Throughout the analysis we assume solar abundances. We also use XSPEC for χ^2 minimization after binning the spectrum to have at least 10 counts/bin. Based on experimentation, we find that χ^2 analysis leads to outcomes similar to Cash statistics. The results of χ^2 statistics are listed in Table 1. We explain below the models in more detail.

Model A: We fit the data with a power law continuum of the form $\phi_E = A\ (\frac{E}{1\ \mathrm{keV}})^{-\Gamma}$, where A is the normalization of the power law at 1 keV, in units of photons cm^{-2} s^{-1} keV^{-1}, and Γ is the X-ray photon index, absorbed by a Galactic column density of $N_{\rm H}^{Gal.} = 2 \times 10^{20}$ cm^{-2} (Lockman & Savage 1995). Both the normalization and the photon index were left as free parameters (Figure 2). The slope was found to be rather flat, $\Gamma = 0.36$, for a QSO, where usually $1.3 < \Gamma < 2.3$ in the observed frame of 0.5-10 keV (Reeves et al. 1997). The flatness of the X-ray slope suggests that there is additional intrinsic absorption.

Model B: We adopt a "normal" QSO continuum, specified by $\Gamma = 1.9$ and $\alpha_{\rm ox} = 1.6$ (Laor et al. 1997), with $\alpha_{ox} = 0.384 \log(f_\nu(2500\ \text{Å})/f_\nu(2\ \mathrm{keV}))$, where $f_\nu(2500$ Å) and $f_\nu(2$ keV) are the rest-frame specific fluxes at 2500 Å and 2 keV, respectively. We attenuate this continuum through an intrinsic neutral absorber, with $N_{\rm H}^{int}$, at z_{em}. We derive the rest-frame $f_\nu(2500$ Å) from its B-magnitude, including the appropriate Galactic dereddening, $E(B-V) = N_{\rm H}^{Gal.}/5.27 \times 10^{21} = 0.09$ (Lockman & Savage 1995), and the k-correction (see Green 1996). The choice of α_{ox} then determines the normalization of the power law at the observed energy of 2 keV$/(1+z)$. In Figure 3, the poor fit at low energies suggests intrinsic absorption, while the bad overall fit indicates that the observed X-ray weakness cannot be explained by absorption alone.

The bad overall fit indicates that PG 1254+047 is both intrinsically X-ray weak and heavily absorbed. The large discrepancy between the data and model is due to the fact that absorption not only decreases the X-ray flux but also deforms the intrinsic spectrum, where the effect is most pronounced at low energies.

Model C: To study the possibility of both intrinsic X-ray weakness and absorption, we remove the constraint that $\alpha_{\rm ox} = 1.6$ and hence allow the normalization of the power law to vary. The fits improve drastically, though not to the extent of giving an acceptable fit ($\chi^2_\nu \approx 1$). We show the results in Figure 4. It is evident that the fit does not strongly support neutral absorption due to the large discrepancy between the data and the models at soft energies. Also, we know that there is no neutral absorber with the above quoted column density because the UV spectra do not contain low-ionization metal lines (Hamann 1998).

Model D: We explore absorption by ionized gas. We hereafter leave the normalization as a free parameter. The amount of absorption depends on the intrinsic total hydrogen column density and the ionization parameter, U, defined as the ratio of the density of hydrogen ionizing photons to that of hydrogen particles ($\mathrm{H^0}$ + $\mathrm{H^+}$). We model the ionized absorber using the photoionization code CLOUDY (Ferland et al. 1998). We generate a grid of QSO continua attenuated through ionized absorbers described by a grid of U and $N_{\rm H}$. The incident continuum is a piecewise powerlaw (Zheng et al. 1996; Laor et al. 1997), which is similar to that used in Hamann (1998). The ultimate results are not critically dependent on the shape the continuum, as long as it in general agreement with that of QSOs (Hamann 1997). We then use XSPEC to interpolate on this grid to find the best fitting model of the observed continuum. Hamann (1998) derived the range of U and $N_{\rm H}$ values that are consistent with the measured BALs (his Figure 7). Larger total $N_{\rm H}$ must be accompanied by large U. For Model D we fix $\log U = 1.2$ to be consistent with both the BAL data and the large X-ray column densities derived here. The resulting fit (Figure 5) improves considerably with $\chi^2_\nu = 0.20$ and $N_{\rm H} = 2.8 \times 10^{23}$ cm^{-2}. The value of A corresponds to an intrinsic (unabsorbed) $\alpha_{\rm ox} = 2.2$, suggesting that PG 1254+047 is intrinsically X-ray weak. We comment more on this in the following section.

Model E: It is similar to Model D, except that we use a steeper powerlaw index of $\Gamma = 2.5$. The final results do not deviate a lot from those of Model D. We experimented with this steep spectrum to see if we can evade the requirement of intrinsic X-ray weakness which the previous models suggested (see discussion below).

For the models with intrinsic absorption (B-E), we also experimented with putting the X-ray absorber at the redshift of the UV absorption lines instead of at the systemic velocity of the QSO. This redshift difference is unresolvable with ACIS. Nonetheless placing the X-ray absorber at z_{abs} leads to lower column densities (by a factor of less than 2).

4. DISCUSSION

4.1. *Intrinsic X-ray Weakness*

The results presented in the previous section require further discussion. They suggest that PG 1254+047 is both intrinsically X-ray weak — intrinsic $\alpha_{\rm ox} = 2.2 \pm 0.1$ obtained after correcting for absorption — and heavily absorbed. Recent observations of other BALQSOs indicate that the X-ray weakness is due to absorption by large column densities (e.g., Brandt et al. 2000; Green et al. 2001; Mathur et al. 2001). In particular, Brandt et al. (2000) discovered an anti-correlation between the the rest-frame equivalent width of C IV$\lambda\lambda$1548, 1550 and $\alpha_{\rm ox}$; strong absorption lines are usually accompanied by an X-ray absorber that steepens α_{ox}. For PG 1254+047, $\alpha_{\rm ox} = 2.6 \pm 0.1$ (uncorrected for intrinsic absorption, Model A in Table 1) and the equivalent width of C IV is ~ 13 Å (Hamann 1998). These values are consistent with the anticorrelation in Brandt et al. (2000).

However, the observed, absorption corrected flux from PG 1254+047, $F(0.2-10\,{\rm keV}) = 5.2\times10^{-14}\,{\rm erg\,s^{-1}\,cm^{-2}}$, is about a factor of 29 below that predicted on the basis of its B-magnitude and $\alpha_{\rm ox} = 1.6$. We have shown in the previous section that no amount of intrinsic absorption was capable of decreasing this amount of intrinsic flux, while at the same time reproducing the overall X-ray spectral shape.

One possible way to decrease the observed X-ray flux without changing α_{ox} is if the X-ray spectrum declines sharply towards higher energies. Mathur et al. (2001) presented a deep ASCA spectrum of the BALQSO PHL 5200, one of the X-ray brightest of its class, and concluded that the X-ray weakness is due to heavy absorption ($N_{\rm H} = 5\times10^{23}\ {\rm cm^{-2}}$) and that the X-ray spectrum is very steep ($\Gamma = 2.5$). We experimented with various values of Γ ranging from 2.5 to 10 while freezing $\alpha_{\rm ox}$ at 1.6, together with intrinsic absorption (neutral and ionized). None of the fits was found to be acceptable; χ^2_ν did not decrease to below ~ 3.5. We note that $\Gamma = 2.5$ and $\alpha_{\rm ox} = 2.0$ lead to satisfactory results ($\chi^2_\nu \approx 0.63$, Model E). Partially covering neutral/ionized absorption (Hamann 1998) also did not lead to significant improvement.

In principle, there is no physical reason that precludes the occurence of intrinsically weak X-ray AGNs. This weakness could be due to time variability, i.e. a QSO caught at an X-ray minimum. For example, Narrow Line Seyfert 1s (NLSy1s) show rapid variability and steep soft X-ray spectra. Mathur (2000) draws the analogy between BALQSOs and NLSy1s arguing that BALQSOs are AGNs in their early evolutionary states, accreting at close to their Eddington limits. Leighly et al. (2001) report a *Beppo*Sax observation of a very bright ($B = 13.9$) QSO, identified from the FIRST survey. PHL 1811 has optical characteristics similar to those of NLSy1s and is extremely X-ray weak with a steep powerlaw slope ($\Gamma = 2.6$). PG 1254+047 could have been observed while it was in a quiescent X-ray state.

X-ray weakness could also be due to the smallness of the X-ray emitting region (Mathur 2000; Leighly et al. 2001). Another possibility for X-ray faintness is that we are actually not seeing all the X-rays coming from the source, but instead the observed X-rays are the small fraction that have been scattered into our line of sight by an electron mirror (Gallagher et al. 1999). To agree with our data, the direct X-rays from the nucleus must be completely absorbed by a Thomson thick absorber, while the scattered X-rays are the ones being attenuated through the ionized absorber. The UV-absorbing gas must be outside of the Thomson thick medium. The relation between the UV and X-ray absorbing gases is discussed below.

4.2. *Wind Dynamics*

Putting the issue of X-ray weakness aside, we can still make important conclusions about the UV/X-ray absorber connection and the physics of wind generation. It is natural to suppose that the X-ray absorption occurs in the outflowing BAL gas (Mathur et al. 1995). However, standard analysis of the BALs, which uses the absorption line troughs to derive optical depths and column densities, typically implies total columns in the range $10^{19} \lesssim N_{\rm H} \lesssim 10^{20}\ {\rm cm^{-2}}$ – two or more orders of magnitude less than the X-ray absorbing columns (Hamann, Korista, & Morris 1993 and references therein)! This enormous discrepancy between the UV and X-ray data must be resolved if we are to reach even a rudimentary understanding of BAL outflows.

All these problems can be addressed by a direct comparison between the UV and X-ray data. Hamann (1998) presented a new analysis of P V$\lambda\lambda$1118, 1128 and other BALs in high-quality HST spectra of PG 1254+047. He used explicit calculations of the column densities and line optical depths under different ionization conditions to show that, if the metals have roughly solar relative abundances, then the significant presence of PV absorption implies that 1) many of the strong lines like C IV, N V and O VI are much more optically thick than they appear, and 2) the total column density in the BAL gas is $N_{\rm H} \gtrsim 10^{22}\ {\rm cm^{-2}}$, considerably larger than previously expected from the depths of the measured troughs. The large column densities and line optical depths are disguised in the observed (moderate-strength) BALs because the absorber does not fully cover the background light source(s) along our line(s) of sight. Our choice of U in Model D leads to an $N_{\rm H}$ that is in agreement with the UV data (Hamann 1998). The UV and X-ray absorbers might, therefore, be identical.

If the UV and X-ray absorption is arising from the same gas, then the total hydrogen column density deduced from the X-rays places additional constraints on the acceleration mechanism of the BAL Region. A relation exists between the terminal velocity of a radiatively accelerated outflow, its column density, and the radius from which it was launched (cf. equation 3 of Hamann 1998). Large column densities require a small launch radius for sufficient radiative acceleration. Substituting values appropriate to PG 1254+047 ($M_{\rm BH} = 10^8\ {\rm M_\odot}$, $L = 10^{46}\ {\rm ergs\ s^{-1}\ cm^{-2}}$, $v_{terminal} = 20,000\ {\rm km\ s^{-1}}$, and $N_{\rm H} = 2.8\times10^{23}\ {\rm cm^{-2}}$), we find that the inner radius is $\sim 10^{16}$ cm. Therefore, the wind is launched from very close to the blackhole. We also calculate the mass loss rate to be $\sim 1\ {\rm M_\odot\ yr^{-1}}$. We use a relation presented in Hamann & Brandt (2001) to derive the hydrogen volume density given U, a radius, and L_{46}. Taking our above values for U (Model D) and L_{46}, and assuming that the BALs form at twice the launch radius, we find that $n_{\rm H} \approx 5\times10^{10}\ {\rm cm^{-3}}$, which yields a BAL region thickness of at least 6×10^{12} cm, using $N_{\rm H}$ from Model D, in agreement with parameters derived for other BALQSOs (Hamann & Brandt 2001).

A very strong constraint from the UV data is the fact that the BALs are detached (Hamann 1998), i.e. the troughs extend from $-15,000$ to $-27,000$ km s^{-1}, with no absorption near the systemic rest velocity. The BALs thus imply that the outflowing gas has already been accelerated to those tremendous speeds. The situation might be like that described Murray et al. (1995), Murray & Chiang (1995) and Elvis (2000). The wind is launched vertically, perpendicular to the accretion disk, and then it bends and flares radially outwards as it is accelerated by radiation pressure from the central engine. The bent geometry provides a natural explaination for detached BAL troughs; lines of sight away from the disk plane can sample portions of the wind that have already been accelerated to the high observed speeds. In the Murray et al. (1995) model, an X-ray absorber, essentially at rest, shields the wind downstream from soft X-rays. This shielding allows the BAL wind to maintain a low enough ionization parameter for substantial resonant line driving and acceleration up to speeds of $\sim 0.1\ c$ (Murray et al. 1995). Alternatively, the wind may be capable of shielding itself (Murray & Chiang 1995; Elvis 2000), in which case the UV and X-ray absorbers are identical and the large column densities we infer from the X-rays must be part of the high velocity wind. The dynamical implication of these large *outflowing* column densities is a small launch radius, as derived above and proposed originally by Murray et al. (1995).

Acknowledgements: We wish to acknowledge support through *Chandra* grants GO 0-1123X and GO 0-1157X. We thank Ian George for comments which improved the presentation, and Keith Arnaud, Niel Brandt, Norman Murray, and Beverley Wills for useful discussion.

REFERENCES

Arav, N., Becker, R. H., Laurent-Muehleisen, S. A., Gregg, M. D., White, R. L., Brotherton, M. S., & de Kook, M. 1999, ApJ, 524, 566
Arnaud, K. A. 1996, Astronomical Data Analysis Software and Systems V, eds. Jacoby G. and Barnes J., p17, ASP Conf. Series volume 101
Brandt, W. N., Laor, A., & Wills, B. J. 2000, ApJ, 528, 637
Elvis, M. 2000, ApJ, 545, 63
Ferland, G., et al. 1998, PASP, 110, 1040
Foltz, C. B., Wilkes, B., Weymann, R., & Turnshek, D. 1983, PASP, 95, 341
Foltz, C. B., Chaffee, F. H., Hewett, P. C., Weymann, R. J., & Morris, S. L. 1990, BAAS, 2, 806
Gallagher, S. C., Brandt, W. N., Sambruna, R. M., Mathur, S., & Yamasaki, N. 1999, ApJ, 519, 549
George, I. A., Turner, T. J., Netzer, H., Nandra, K., Mushotzky, R. F., & Yaqoob, T. 1998, ApJS, 114, 73
Gould, A., Bahcall, J. N., & Maoz, D. 1993, ApJS, 88, 53
Green, P. J., Aldcroft, T. L., Mathur, S., Wilkes, B. J, & Elvis, M. 2001, ApJ accepted, astro-ph/0105258
Hamann, F., Korista, K. T., & Morris, S. L. 1993, ApJ, 415, 541
Hamann, F. 1997, ApJS, 109, 279
Hamann, F. 1998, ApJ, 500, 798
Hamann, F., & Brandt, W. N. 2001, in prep.
Kirhakos, S., et al. 1994, PASP, 106, 646
Laor, A., et al. 1997, ApJ, 477, 93
Leighly, K. M., Halpern, J. P., Helfand, D. J., Becker, R. H., & Impey, C. D. 2001, AJ, in press
Lockman, F. J., & Savage, B. D. 1995, ApJS, 97, 1
Mathur, S., Elvis, M., & Singh, K. 1995, ApJ, 455, L9
Mathur, S. 2000, MNRAS, 314, L17
Mathur, S., Matt, G., Green, P. J., Elvis, M., Singh, K. P. 2001, ApJ, in press
Murray, N., & Chiang, J. 1995, ApJ, 454, L101
Murray, N., Chiang, J., Grossman, J. A., & Voit, G. M. 1995, ApJ, 451, L498
Netzer, H. 1996, ApJ, 473, 781
Reeves, J. N., et al. 1997, MNRAS, 292, 468
Reynolds, C. S. 1997, MNRAS, 286, 513
Turner, T. J., Weaver, K. A., Mushotzky, R. F., Holt, S. S., & Madejski, G. M., 1991, ApJ, 381, 85
Wang, T. G., Wang, J. X., Brinkmann, & Matsuoka, M. 1999, ApJ, 519, L35
Weymann, R. J., Morris, S. L., Foltz, C. B., & Hewett, P. C. 1991, ApJ, 373, 23
Wilkes, B. J., Tananbaum, H., Worral, D. M., Avni, Y., Oey, M. S. & Flanagan, J. 1994, ApJS, 92, 53
Zheng, W., et al. 1996, ApJ, 475, 469

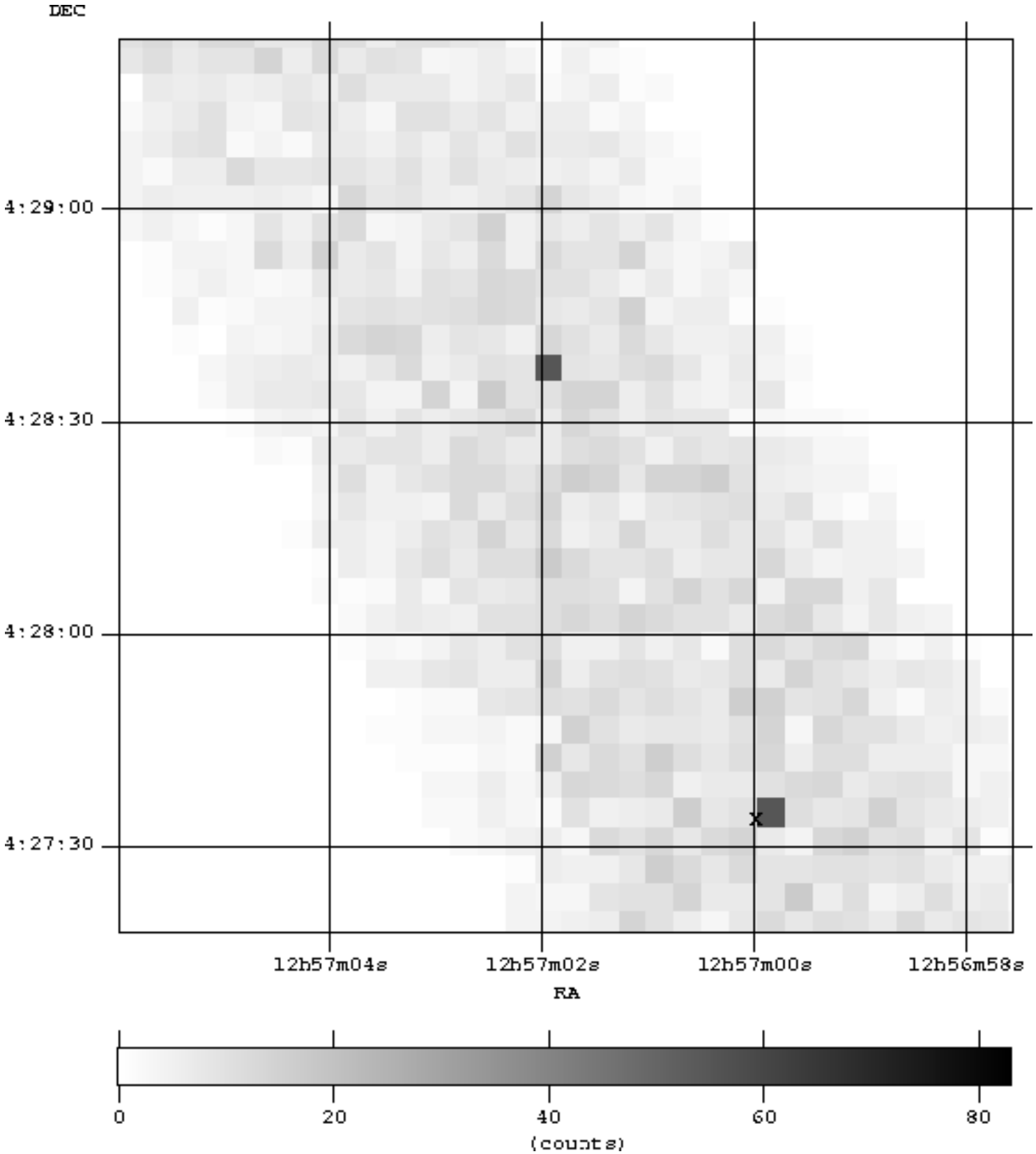

FIG. 1.— ACIS image of PG 1254+047. PG 1254+047 is the darkest pixel nearest to $\alpha(\mathrm{J2000}) = 12^h57^m00^s$. The "X" symbol denotes the optical position of the QSO, within $1''$of the X-ray position. The other dark pixel is $\sim 13''$ from a visual source reported in Kirhakos et al. (1994).

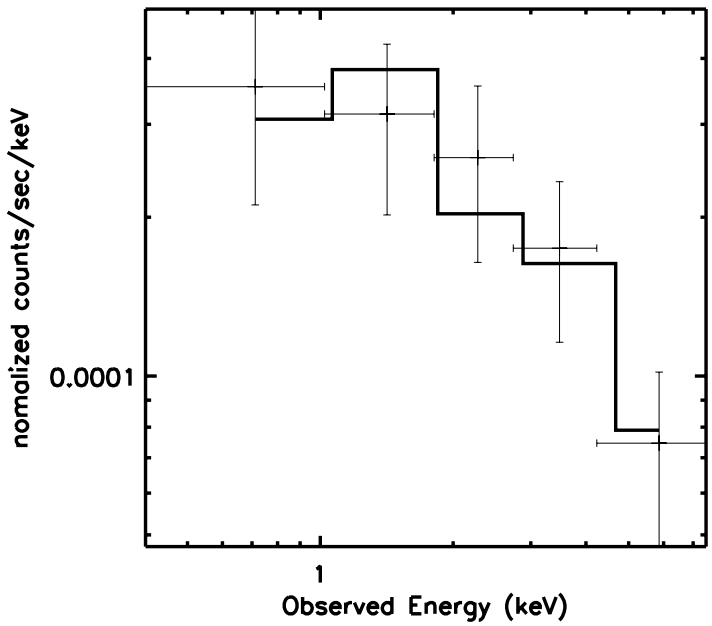

FIG. 2.— Model A: Galactic Absorption only with free normalization. The crosses represent the data binned to provide 10 counts per bin. The solid histogram is the fit. The fit yields $A = 6.47 \times 10^{-7}$ photon s^{-1} cm^{-2} keV^{-1} at 1 keV, and $\Gamma = 0.36$, for $\chi^2_\nu = 0.29$ and 3 degrees of freedom (d.o.f.).

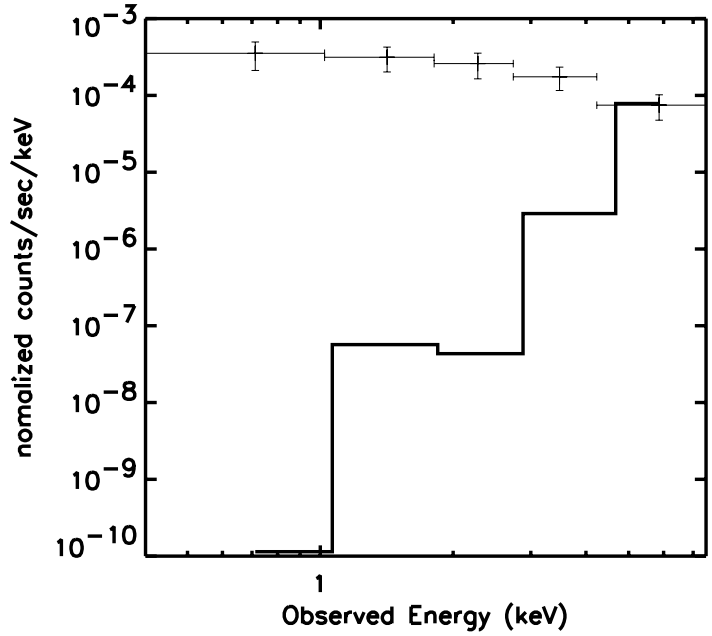

FIG. 3.— Model B: Neutral Absorber and fixed normalization. $N_H = 5.01 \times 10^{24} cm^{-2}$, $\chi^2_\nu = 7.50$ for 4 d.o.f.

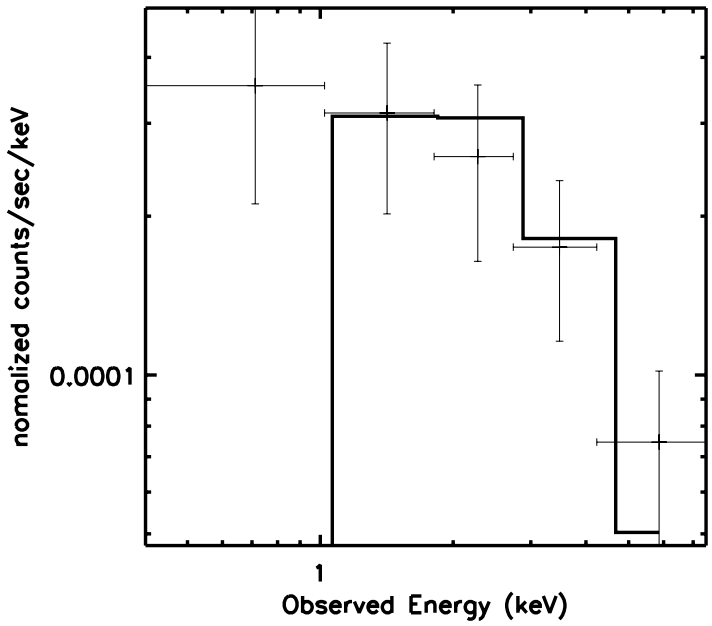

FIG. 4.— Model C: Neutral Absorber and free normalization. $N_H = 10.81 \times 10^{22}\mathrm{cm}^{-2}$, $A = 5.86 \times 10^{-6}$ photon s^{-1} cm^{-2} keV^{-1} at 1 keV, $\chi^2_\nu = 2.28$ for 3 d.o.f.

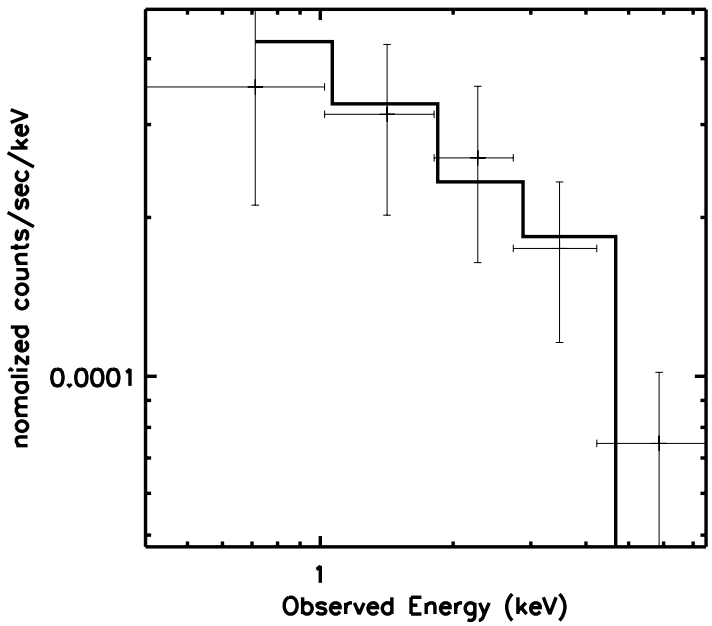

FIG. 5.— Model D: Ionized Absorber. $N_H = 2.8 \times 10^{23}\mathrm{cm}^{-2}$, $\log U = 1.2$, $A = 8 \times 10^{-6}$ photon s^{-1} cm^{-2} keV^{-1} at 1 keV, $\chi^2_\nu = 0.20$ for 3 d.o.f.

TABLE 1
SPECTRAL FIT PARAMETERS[a]

Model	$\log U$	$N_{\rm H}$ (10^{22} cm^{-2})	A^b	Γ	α_{ox}	χ^2_ν
A	—	—	$0.7^{+0.2}_{-0.3}$	$0.36^{+0.42}_{-0.44}$	2.6 ± 0.1	0.29 for 3 d.o.f[e]
B	neutral	501[d]	240[c]	1.9[c]	1.6[c]	7.50 for 4 d.o.f
C	neutral	10.8[d]	5.9[d]	1.9[c]	2.2[d]	2.28 for 3 d.o.f
D	1.2[c]	28^{+3}_{-4}	8 ± 3	1.9[c]	2.2 ± 0.1	0.20 for 3 d.o.f
E	1.2[c]	28^{+2}_{-4}	17 ± 7	2.5[c]	2.0 ± 0.1	0.63 for 3 d.o.f

[a] All errors are at the 90% confidence level.
[b] In units of 10^{-6} photon s^{-1} cm^{-2} keV^{-1}.
[c] Fixed parameter.
[d] Confidence levels not quoted since $\chi^2_\nu > 2$.
[e] degrees of freedom.

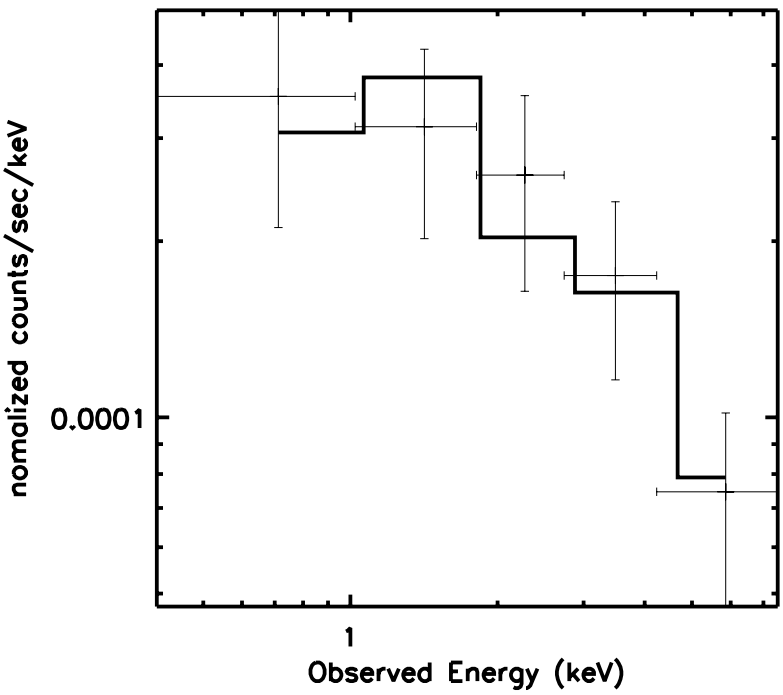
nomalized counts/sec/keV
0.0001
1
Observed Energy (keV)

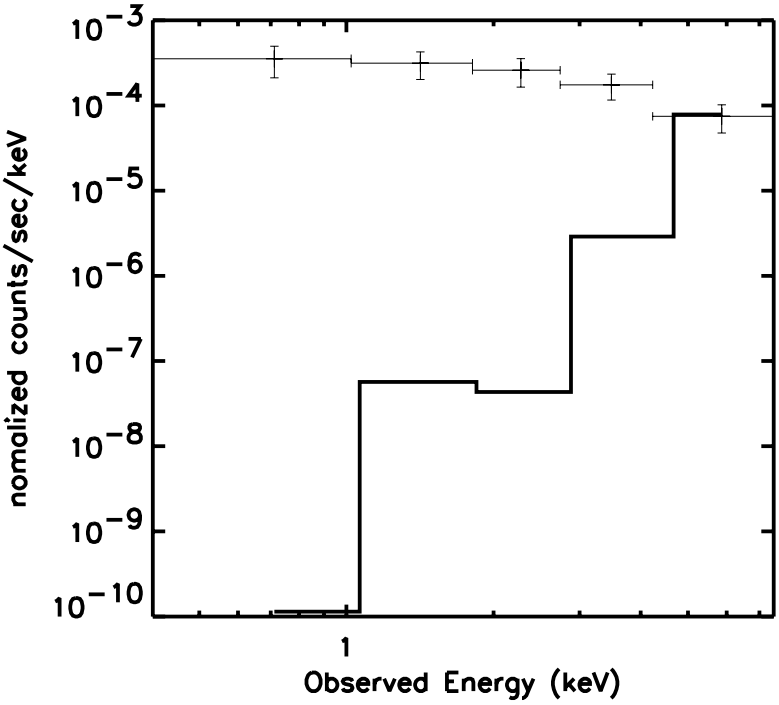
10^{-3}
10^{-4}
10^{-5}
10^{-6}
10^{-7}
10^{-8}
10^{-9}
10^{-10}
nomalized counts/sec/keV
1
Observed Energy (keV)

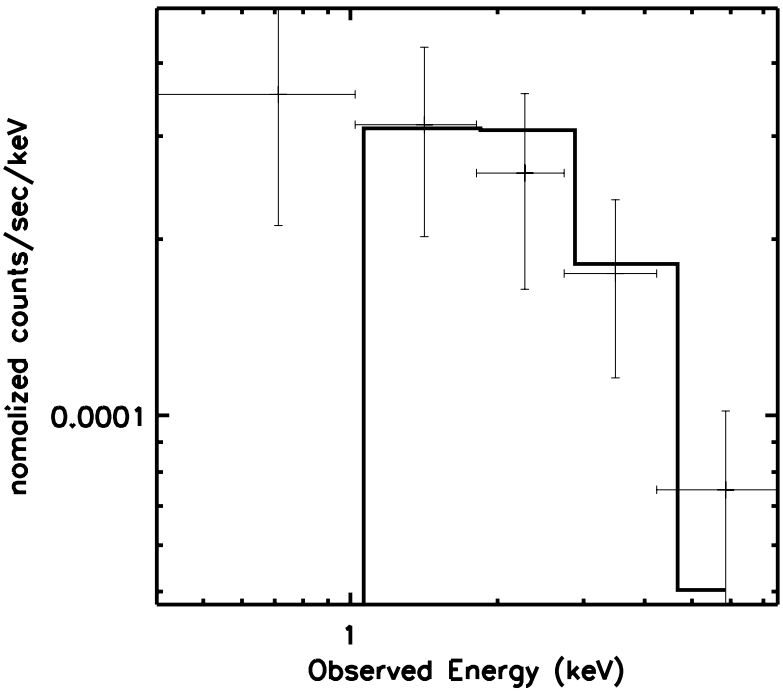
nomalized counts/sec/keV
0.0001
1
Observed Energy (keV)

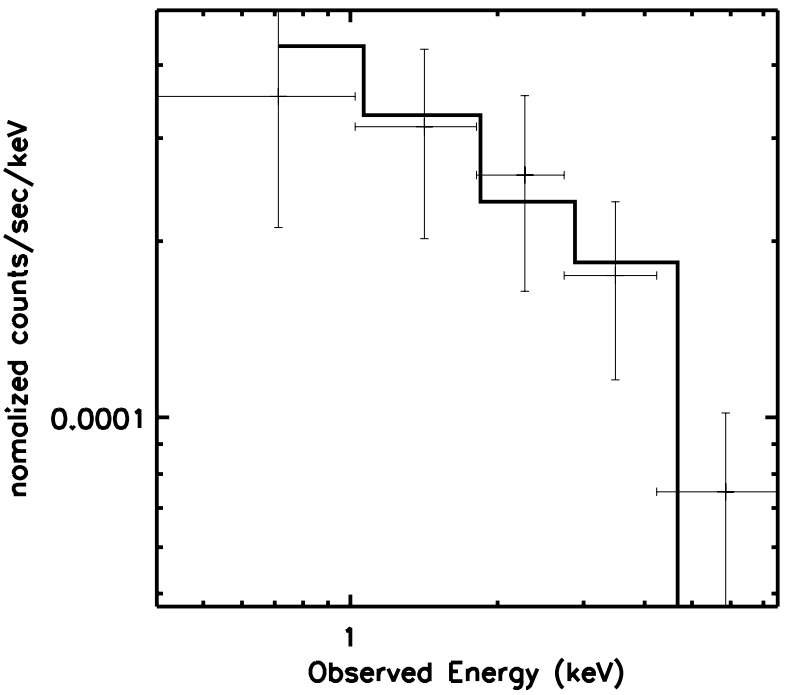
nomalized counts/sec/keV
0.0001
1
Observed Energy (keV)